

CODEN STJSAO
ZX470/1570ISSN 0562-1887
UDK 82(03)=65-32-45

Compliance Analysis of an Articulated Machining Robot

*Nikola SLAVKOVIĆ,
Saša ŽIVANOVIĆ,
Dragan MILUTINOVIĆ and
Miloš GLAVONJIĆ*

Mašinski fakultet, Univerzitet u Beogradu
(Faculty of Mechanical Engineering,
University of Belgrade), Kraljice Marije 16,
11120 Beograd, Republic of Serbia

dmilutinovic@mas.bg.ac.rs

Keywords

*Robot
Machining
Compliance analysis*

Ključne riječi

*Robot
Obrada
Analiza popustljivosti*

Primljeno (Received): 2011-10-10

Prihvaćeno (Accepted): 2012-02-07

1. Introduction

Industrial robots are promising cost-effective and flexible alternative for certain multi-axis milling applications. Compared to machine tools, robots are cheaper and more flexible with larger workspace. It is well known that poor accuracy, stiffness and complexity of programming are the most important limiting factors for wider adoption of robotic machining in machine shops [1].

Stiffness or compliance modeling and analysis in robotic machining have attracted attention of many researches [1-7]. As stated in [1] the major position error sources in robotic machining can be classified into two categories: (i) cutting force induced errors, and (ii) motion errors (e.g., kinematic, dynamic, etc.).

Motion errors, typically in the range of 0.1 mm, are inherent and rooted in the robot position controller, and they would appear even in non-contact tasks. As milling cutting forces are of several hundred N, the force-induced errors could easily exceed 1 mm. The latter statement is quite logical because the stiffness for typical articulated robots is usually less than 1 N/ μm , while standard CNC machine tools often have stiffness

Original scientific paper

This paper describes analytically and experimentally based compliance modeling and identification of 5-axis vertical articulated machining robot. The conventional method for the calculation of Cartesian space compliance based on joint compliances and Jacobian matrix is expanded and used for experimental 5-axis machining robot. Analytical analysis was conducted for effects of compliances of each joint individually on Cartesian space robot compliance. Experimentally, the Cartesian space compliance is obtained by direct measurement of the absolute displacements evoked by static forces along 3- orthogonal directions at the tool tip in the robot workspace for the case of 3-axis machining.

Analiza popustljivosti robota za obradu vertikalne zglobne konfiguracije

Izvorno znanstveni članak

U radu su predstavljeni analitičko i eksperimentalno modeliranje i identifikacija popustljivosti 5-osnog robota za obradu vertikalne zglobne konfiguracije. Konvencionalni pristup za određivanje popustljivosti robota u Kartezijevom prostoru, zasnovan na popustljivosti zglobova i Jakobijan matrici je proširen i upotrebljen za određivanje popustljivosti eksperimentalnog 5-osnog robota. Analitička analiza je provedena s ciljem definiranja utjecaja popustljivosti svakog zgloba pojedinačno na popustljivost robota u Kartezijevom prostoru. Popustljivost robota u Kartezijevom prostoru je eksperimentalno određena direktnim mjerenjem apsolutnih pomicanja vrha robota izazvanih statičkom silom u sva tri ortogonalna pravca u radnom prostoru za slučaj 3-osne obrade.

values greater than 50 N/ μm . Similar statements are also given in [3].

The sources that determine the stiffness of a typical robot manipulator are the compliance of its joints, actuators and other transmission elements, geometric and material properties of the links, base, and the active stiffness provided by its position control system. For the purpose of this research, we assume that the compliance of the actuators and of the transmission elements is the dominant source of the stiffness, and it can be represented by a linear torsional spring for each joint, while the links are infinitely stiff.

Unlike multi-axis CNC machine tools, robot tool tip displacements are coupled and varied even when subjected to the same force at different workspace locations. Such coupling results in displacements not only in the direction of the reaction force, but can also generate some counter-intuitive results. Mainly, three kinds of deviations occur due to the compliance of a machining robot during high speed cutting: static displacement, low frequency and high frequency oscillations. In this paper, the static displacements which have the highest impact on overall cutting accuracy are analyzed.

<u>Symbols/Oznake</u>	
A	- 4x4 transformation matrix - 4x4 transformacijska matrica
a	- D-H kinematic parameter, mm - D-H kinematički parametar
C_x	- 5x5 Cartesian space compliance matrix - 5x5 matrica popustljivosti u Kartezijevom prostoru
C_θ	- 5x5 diagonal joint compliance matrix - 5x5 dijagonalna matrica popustljivosti zglobova
d	- D-H kinematic parameter, mm - D-H kinematički parametar
F	- 3x1 static force vector, N - 3x1 vektor statičke sile
J	- 5x5 Jacobian matrix - 5x5 Jakobijeva matrica
J	- 5x1 column vector of Jacobian matrix - 5x1 vektor kolone Jakobijeve matrice
i, j, k	- unit vectors - jedinični vektori
l_T	- tool length, mm - dužina alata
P	- 3x1 position vector, mm - 3x1 vektor položaja
$\{M\}$	- robot reference frame - referentni koordinatni sistem robota
$\{T\}$	- tool frame - koordinatni sistem alata
T	- 4x4 transformation matrix - 4x4 transformacijska matrica
x	- 5x1 world coordinate vector - 5x1 vektor vanjskih koordinata
<u>Greek letters/Grčka slova</u>	
α	- D-H kinematic parameter, deg - D-H kinematički parametar
δx	- 3x1 linear displacement vector, mm - 3x1 vektor translatorskih pomaka
θ	- D-H kinematic parameter, deg - D-H kinematički parametar
θ	- 5x1 joint coordinates vector, deg - 5x1 vektor unutrašnjih koordinata
<u>Subscripts/Indeksi</u>	
i	- joint number - broj zgloba
n	- number of joints - broj zglobova
M	- machine - stroj
T	- tool - alat

In order to contribute to efficient use of robots for machining applications, research and development of reconfigurable robotic machining system were initiated. The research and development comprise two groups of problems: the realization of a specialized 5-axis machining robot with integrated motor spindle in order to improve robotic machining accuracy, and the development of the machining robot control and programming system which can be directly used by CNC machine tool programmers and operators [8].

This paper describes analytically and experimentally based compliance modeling and analysis of 5-axis machining robot. The conventional method for the calculation of Cartesian space compliance based on joint compliances and Jacobian matrix [4,6,7] is expanded and used. Analytical analysis was conducted for effects of compliances of each joint individually on Cartesian space robot compliance. Experimentally, the Cartesian space compliance is obtained by direct measurement of the absolute displacements evoked by static forces along 3- Cartesian directions at the tool tip in the robot workspace for the case of 3-axis milling.

2. Problem statement

A basic module of the proposed concept of the robotic machining system [5] is the specialized 5-axis robot, Figure 1, with integrated motor spindle and with larger workspace, higher payload and stiffness. Due to its advantages in respect of stiffness and singularities, such robot would operate as a specific vertical 5-axis milling machine (X, Y, Z, A, B) spindle-tilting type. The development of specialized 5-axis vertical articulated machining robot is a joint project with robot manufacturer.

For the development of control and programming system as well as for the analysis and development of the mechanical structure of 5-axis machining robot from Figure 1, a 6-axis vertical articulated robot with payload of 50 kg, Figure 2, was used as a testbed, in a way that the sixth axis was blocked. The robot is equipped with high speed motor spindle with maximum speed of 18,000 min⁻¹.

The focus of current research, one part of results being presented in this paper, is related to compliance modeling and analysis of the experimental 5-axis machining robot, which includes:

- Analytically based robot compliance modeling,
- Experimentally based robot compliance identification.

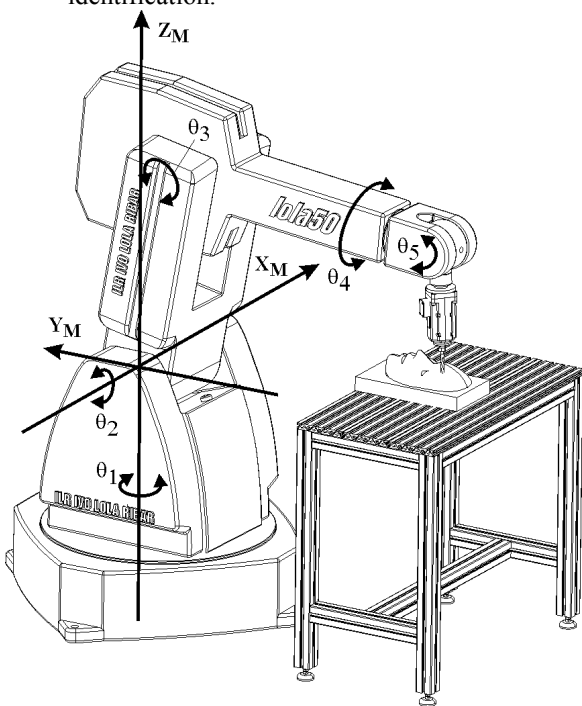


Figure 1. 5-axis machining robot

Slika 1. 5-osni robot za obradu

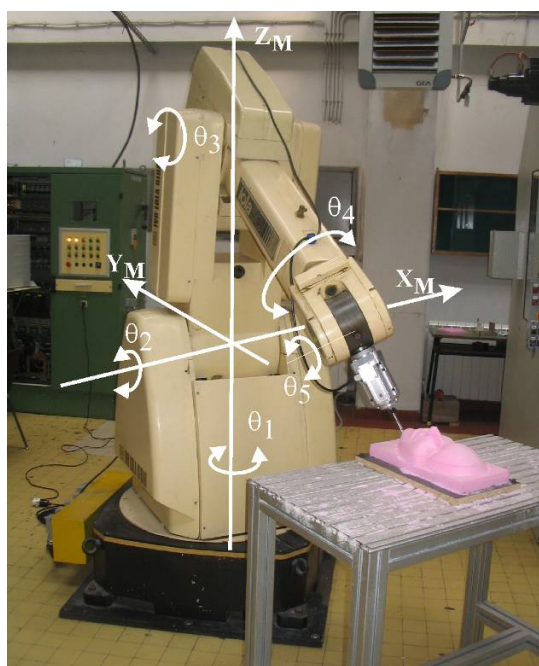


Figure 2. Experimental 5-axis machining robot

Slika 2. Eksperimentalni 5-osni robot za obradu

3. Jacobian matrix and workspace

As it was mentioned, the 5-axis robot from Figure 1 will be considered here as a specific configuration of the 5-axis vertical milling machine (X, Y, Z, A, B) spindle-tilting type. Figure 3 represents a geometric model of the robot.

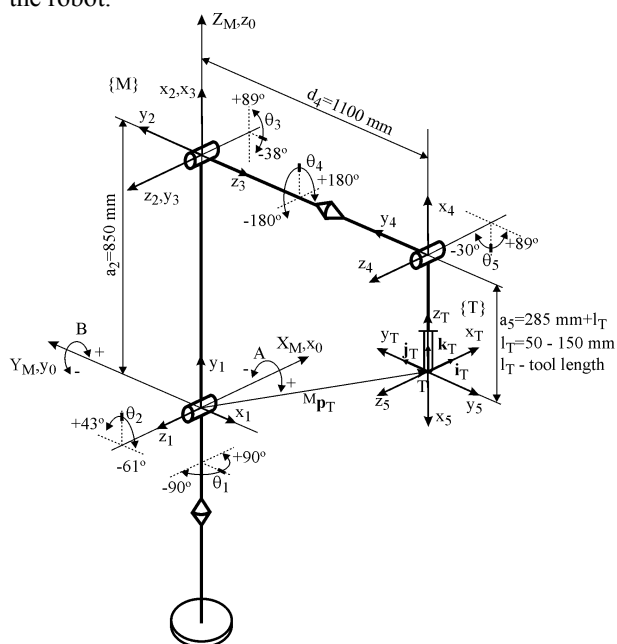


Figure 3. D-H link coordinate frames

Slika 3. D-H koordinatni sustavi segmenata

The robot reference frame $\{M\}$ has been adopted according to the standard of this machine type and coincides with the robot based frame (x_0, y_0, z_0) . The tool frame $\{T\}$ is attached to the milling tool tip T in a way that axis z_T coincides with tool axis and also coincides with axis of the last link of the robot to which motor spindle is attached. The thus configured machining robot, where machining is performed on a work table in front of the robot as well as limited motions in joints relative to the reference position allows for: taking into account only one solution of inverse kinematic, avoiding the robot singularities, conveniences related to the stiffness.

Joint coordinates vector for this 5-axis vertical articulated robot is represented as $\theta = [\theta_1 \ \theta_2 \ \theta_3 \ \theta_4 \ \theta_5]^T$ where θ_i are scalar joint variables controlled by actuators. Given that the robot has 5 DOF, only the direction of tool axis z_T is controllable, while axes x_T and y_T will have uncontrollable rotation about it. The position and orientation of the tool frame $\{T\}$ relative to robot reference frame $\{M\}$ is described by world coordinates vector expressed as $\mathbf{x} = [X_M \ Y_M \ Z_M \ A \ B]^T$.

To model the robot, the Denavit-Hartenberg (D-H) notation [9] was used. To perform kinematic analysis, first coordinate frames are rigidly attached to each link. The homogeneous transformation describing the relation between one link and the next link is traditionally referred to as an A matrix. Matrix ${}^{i-1}_i A$ designates D-H transformation matrix relating frame (i) to frame ($i-1$). Figure 3 shows D-H coordinate frames for the experimental 5-axis robot from Figure 2 in the reference position taking into account the ranges of joint motions.

Table 1 shows link kinematic parameters for the experimental 5-axis robot.

Table 1. D-H link kinematic parameters

Tablica 1. D-H kinematički parametri

link i / segment i	α_i [°]	a_i [mm]	d_i [mm]	θ_i [°]
1	90	0	0	$\theta_1 - 90$
2	0	a_2	0	$\theta_2 + 90$
3	90	0	0	θ_3
4	-90	0	d_4	$-\theta_4$
5	0	a_5	0	$\theta_5 + 180$

Substituting D-H parameters of the links the transformation matrices ${}^{i-1}_i A$ are obtained first. As noticeable from Figure 3 the frame $\{T\}$ can be described relative to the frame (x_5, y_5, z_5) by homogeneous transformation matrix as ${}^5_T T$ [8]. Now, as it is well-known [9], the tool position and orientation i.e. the position and orientation of frame $\{T\}$ with respect to the robot reference frame $\{M\}$, Figure 3, for the given joint coordinates vector θ and specified link parameters can be determined as

$${}^M_T T = {}^0_1 A \cdot {}^1_2 A \cdot {}^2_3 A \cdot {}^3_4 A \cdot {}^4_5 A \cdot {}^5_T T \quad (1)$$

The position and orientation of arbitrary frame i attached to the link i with respect to the robot reference frame $\{M\}$ i.e. robot based frame (x_0, y_0, z_0) can be expressed as

$${}^0=M_i T = {}^0_1 A \cdot {}^1_2 A \cdot \dots \cdot {}^{i-1}_i A = \prod_{j=1}^i {}^{j-1}_j A = \begin{bmatrix} {}^{i-1}_i \mathbf{i}_i & {}^{i-1}_i \mathbf{j}_i & {}^{i-1}_i \mathbf{k}_i & | & {}^{i-1}_i \mathbf{p}_{O_i} \\ 0 & 0 & 0 & | & 1 \end{bmatrix} \quad (2)$$

for $i = 1, 2, 3, \dots, n = 5$ where n is number of joints.

The robot Jacobian matrix relates joint velocities to Cartesian velocities of the tool tip. The mapping between static forces applied to the end-effector and resulting torques at the joints can also be described by Jacobian matrix [9,10]. Considering that the robot

consists of five revolute joints, the Jacobian matrix has as many rows as there are degrees of freedom and the number of columns is equal to the number of joints

$$J = [J_1 \quad J_2 \quad \dots \quad J_n] \quad (3)$$

with column vectors

$$J_i = \begin{bmatrix} {}^i \mathbf{k}_{i-1} \times ({}^0 \mathbf{p}_n - {}^0 \mathbf{p}_i) \\ {}^0 \mathbf{k}_{i-1} \end{bmatrix} \quad (4)$$

Substituting vectors from equation (2) in equation (4) Jacobian matrix columns J_i , $i = 1, 2, 3, \dots, n = 5$ are obtained.

Workspace for 3-axis machining is shown in Figure 4.

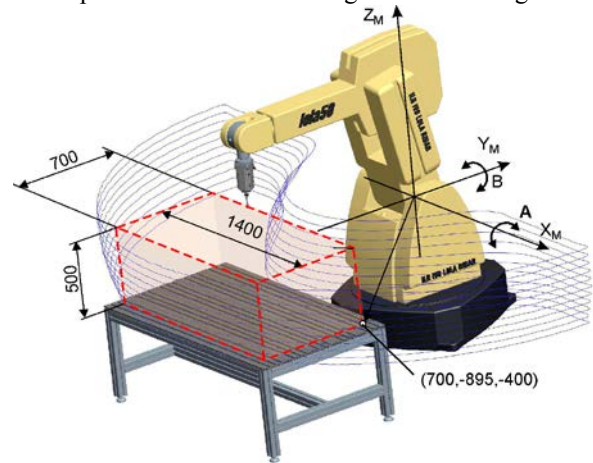


Figure 4. Workspace in the case of 3-axis machining ($A=0^\circ$, $B=0^\circ$)

Slika 4. Radni prostor robota za slučaj 3-osne obrade ($A=0^\circ$, $B=0^\circ$)

4. Compliance modeling

As stated in [1,2,3,5] elastic properties of robot segments are insignificant, so there follows below the analysis of compliance model in Cartesian space based on joint compliances. The analysis will be conducted on the existing experimental machining robot from Figure 2.

Based on the principle of virtual work, the convectional formulation for the mapping of joint compliance matrix C_θ into the Cartesian space compliance matrix $C_X(\theta)$ [4,5,7] is expressed as

$$C_X(\theta) = J(\theta) \cdot C_\theta \cdot J(\theta)^T \quad (5)$$

where C_θ is the compliance matrix in joint space which has the diagonal form as

$$C_\theta = \text{diag}(C_{\theta_1}, \dots, C_{\theta_n}) \quad (6)$$

and $J(\theta)$ is Jacobian matrix.

Equation (5) is practically used in [7] to determine the robot compliance center and in [5] for machining robot compliance analysis where it is stated how suitable it is, for it allows mapping of the joint compliance matrix C_θ into Cartesian compliance matrix $C_X(\theta)$ without calculating any inverse kinematic functions. Since C_θ is diagonal matrix, the Cartesian space compliance matrix $C_X(\theta)$, equation (5), is the sum of the joint compliances associated with each individual joint as

$$C_X(\theta) = C_{X1}(C_{\theta1}) + \dots + C_{Xn}(C_{\thetan}), \quad n = 5 \quad (7)$$

where

$$C_{Xi}(C_{\theta i}) = C_{\theta i} \cdot \mathbf{J}_i \cdot \mathbf{J}_i^T, \quad i = 1, 2, \dots, n, \quad n = 5 \quad (8)$$

while \mathbf{J}_i are column vectors of Jacobian matrix $J(\theta)$.

Equations (7) and (8) provide insight into the impact of compliance of each joint individually on the Cartesian space compliance. This means that impact of the corresponding joint is obtained incorporating in the equation (7) only its compliance, while the other joints are considered stiff. This is of crucial importance for the present paper, because it can be useful for robot manufacturer's experts in the design of specialized machining robot [11,12].

For an articulated robot, $C_X(\theta)$ is symmetric non-diagonal and configuration dependent matrix. Thus, if C_θ can be experimentally determined, the Cartesian space compliance matrix $C_X(\theta)$, equation (5) and the linear displacement of robot tool tip under external static force vector $\mathbf{F} = [F_x \ F_y \ F_z]^T$ at any location in the workspace can be estimated as

$$\delta \mathbf{x} = C_X(\theta) \cdot \mathbf{F} \quad (9)$$

Experimental determination of compound joint compliances was performed by robot manufacturer's experts, and are given in Table 2.

Table 2. Experimentally identified joint compliance

Tablica 2. Eksperimentalno određene popustljivosti zglobova

Joint number i / Broj zgloba i	1	2	3	4	5
$C_{\theta i} [\text{rad/Nm}] \cdot 10^{-7}$	7,14	10,12	12,30	17,32	91,35

Using experimentally determined joint compliances, the Cartesian space compliance matrix is calculated in workspace shown in Figure 4.

Figure 5 shows the distributions of analytically determined compliances in the $Z_M = 0$ plane.

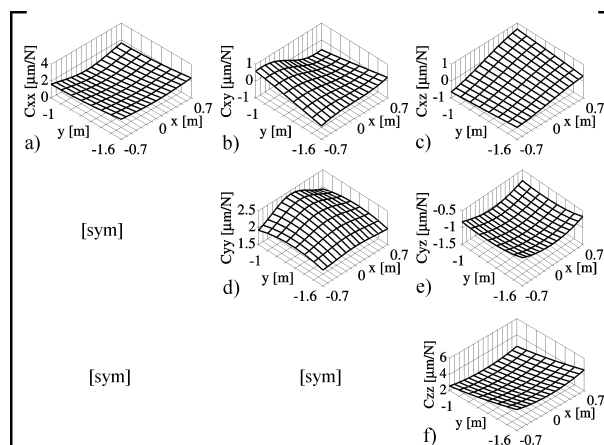


Figure 5. Distributions of analytical compliances in the plane $Z_M=0$

Slika 5. Distribucije analitički određenih popustljivosti u ravnini $Z_M=0$

Figure 5 can be also viewed as the Cartesian space compliance matrix $C_X(\theta)$ in the $Z_M = 0$ plane in the workspace shown in Figure 4.

The distributions of direct-compliances C_{xx}, C_{yy} and C_{zz} are presented in Figures 5a, 5d and 5f respectively. The distributions of cross-compliances C_{yx}, C_{zx} and C_{zy} are given in Figs. 5b, 5c and 5e respectively.

The distributions of dominant components of direct-compliances originating from individual joints are shown in Figure 6.

5. Experimental compliance

Another approach to obtain the Cartesian compliance of the machining robot is the direct measurement of the absolute displacement evoked by a load at the tool tip.

The elements of the experimental setup are shown in Figure 7. The original and deformed positions of sphere-tip tool caused by deadweight of 250N are measured with FARO Portable CMM 3D, from which translational displacements $\delta x, \delta y$ and δz are calculated.

Displacements of the sphere-tip tool are measured in the workspace shown in Figure 4 at 40 points with the fixed X_M - and Y_M -coordinates in 6 Z_M -levels ($Z_M = -400\text{mm}$ to $Z_M = 100\text{mm}$). Experimental compliances are determined based on sphere-tip tool displacements evoked by static amount of the milling force of 250N in all 3 Cartesian directions, Figure 7.

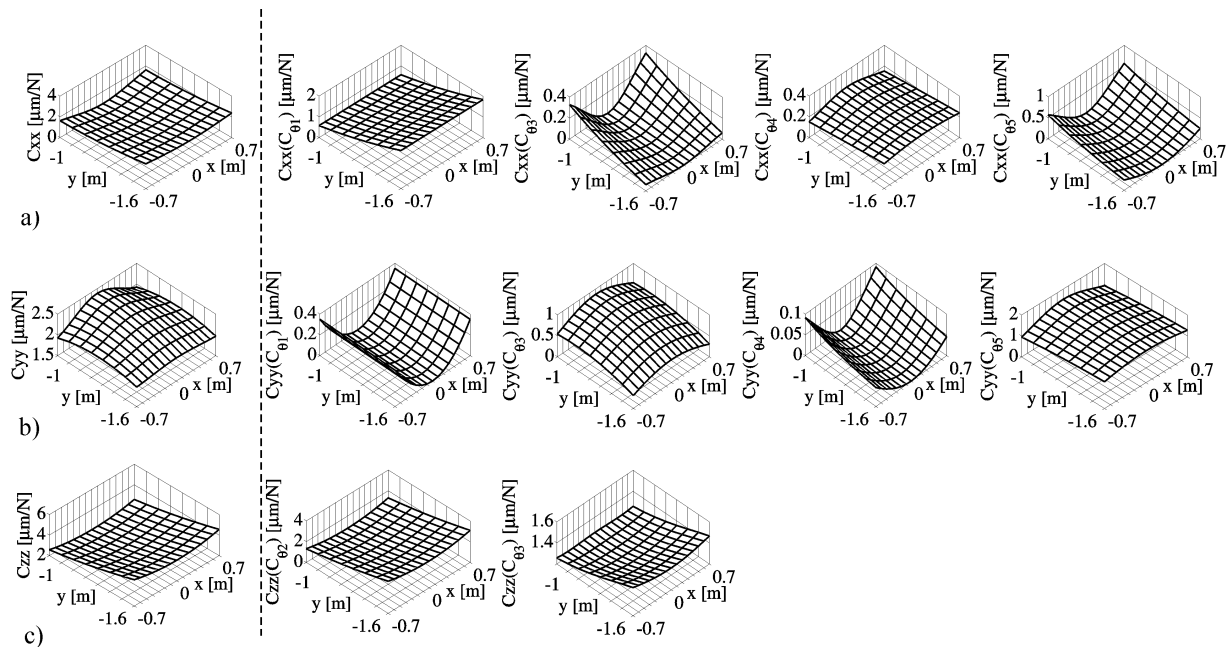


Figure 6. Distributions of dominant direct-compliance components

Slika 6. Distribucije najutjecajnijih komponenti direktnih popustljivosti

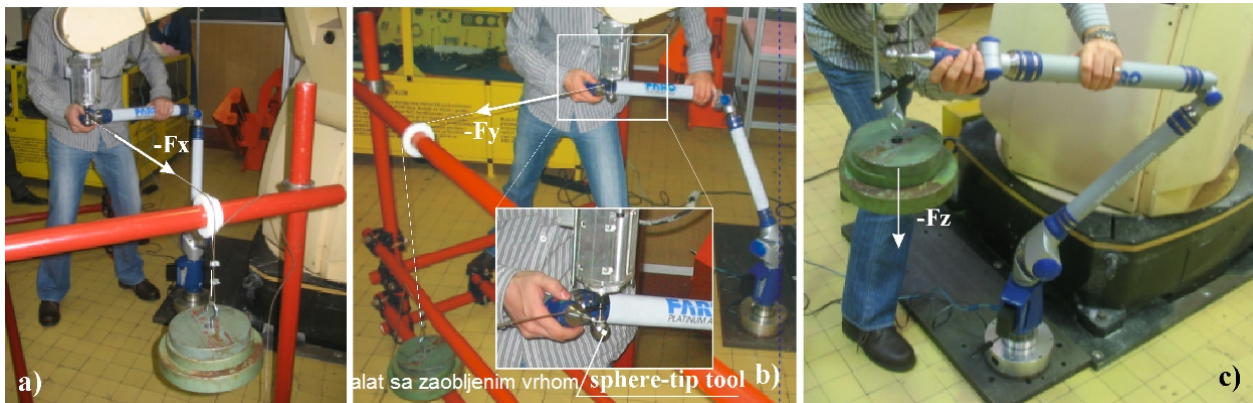


Figure 7. Experimental setup of robot loading and displacements measurement

Slika 7. Eksperimentalno mjerenje pomicanja vrha robota

Figure 8 shows the distributions of experimentally obtained compliances in the $Z_M = 0$ plane. The distributions of experimental direct-compliances C_{xx} , C_{yy} and C_{zz} are shown in Figures 8a, 8e and 8i, respectively. Experimental cross-compliances are presented in Figures 8b, 8c and 8f, respectively. Comparing them with analytically determined compliances, Figure 5, it can be inferred that the character of their distributions is similar, but experimentally determined compliances are slightly higher. Higher values of experimentally determined compliances compared to those determined analytically originate from compliances of structure elements, motor spindle and tool itself.

6. Conclusion

The paper presents analytically and experimentally based compliance modeling and analysis of 5-axis machining robot based on conventional approach for the mapping of joint compliances into robot Cartesian space compliance. By expanding this modeling approach, it has been shown that it is possible to analyze each joint compliance impact on robot Cartesian space compliance. Satisfactory correlation between analytically and experimentally determined robot Cartesian space compliances confirms the usability of each joint compliance effects on tool tip displacements. Suitable model of the process forces and compliance

model proposed in this paper also enable the development of virtual robotic machining system for further research [13,14]. The present research has laid foundations for an advanced design method for one machining robot as well as for the development of strategy for real-time tool tip displacement compensation based on captured process forces.

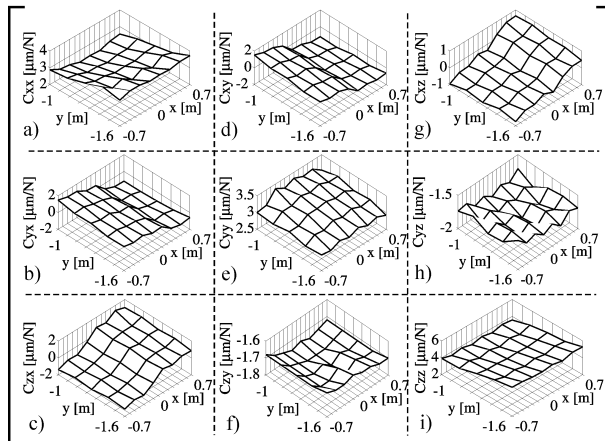


Figure 8. Distributions of experimental compliances in the plane $Z_M=0$

Slika 8. Distribucije eksperimentalno određenih popustljivosti u ravnini $Z_M=0$

Acknowledgements

The authors would like to thank the Ministry of Education and Science of Serbia for providing financial support that made this work possible.

REFERENCES

- [1] PAN, Z.; ZHANG, H.: *Robotics machining from programming to process control: a complete solution by force control*, Industrial Robot: An International Journal, 35 (2008) 5, 400-409.
- [2] ALICI, G.; SHIRINZADEH, B.: *Enhanced stiffness modeling, identification and characterization for robot manipulators*, IEEE Transactions on Robotics, 21 (2005) 4, 554-564.
- [3] ABELE, E.; ROTHENBUCHER, S.; WEIGOLD, M.: *Cartesian compliance model for industrial robots using virtual joints*, Production Engineering, 2 (2008) 3, 339-343.
- [4] HUDGENS, J.C.; HERNANDEZ, E.; TESAR, D.: *A compliance parameter estimation method for serial manipulator*, DSC Applications of Modeling and Identification to Improve Machine Performance ASME, 29 (1991), 15-23.
- [5] ABELE, E.; WEIGOLD, M.; ROTHENBUCHER, S.: *Modeling and identification of an industrial robot for machining application*, Annals of the CIRP, 56 (2007) 1, 387-390.
- [6] DUMAS, C.; CARO, S.; GARNIER, S.; FURET, B.: *Joint stiffness identification of six-revolute industrial serial robots*, Robotics and Computer-Integrated Manufacturing, 27 (2011) 4, 881-888.
- [7] MILUTINOVIĆ, D.; MILAČIĆ, V.: *Micro scara robot as universal adaptive compliant wrist*, Annals of the CIRP, 45 (1996) 1, 31-34.
- [8] MILUTINOVIĆ, D.; GLAVONJIĆ, M.; SLAVKOVIĆ, N.; DIMIĆ, Z.; ŽIVANOVIĆ, S.; KOKOTOVIĆ, B.; TANOVIĆ, LJ.: *Reconfigurable robotic machining system controlled and programmed in a machine tool manner*, International Journal of Advanced Manufacturing Technology, 53 (2011) 9-12, 1217-1229.
- [9] FU K.S.; GONZALEZ R.C.; LEE C.S.G.: *Robotics: control, sensing, vision, and intelligence*, McGraw-Hill, New York, 1987.
- [10] SCIAVICCO, L.; SICILIANO, B.: *Modelling and Control of Robot Manipulators*, 2nd ed., Springer-Verlag, London, 2000.
- [11] MILUTINOVIĆ, D.; GLAVONJIĆ, M.; SLAVKOVIĆ, N.; ŽIVANOVIĆ, S.; KOKOTOVIĆ, B.; DIMIĆ, Z.: *Compliance modeling and identification of 5-axis vertical articulated robot for machining applications*, 34th International Conference on Production Engineering-Proceedings, Nis 2011, 381-384.
- [12] MILUTINOVIĆ, D.; GLAVONJIĆ, M.; SLAVKOVIĆ, N.; ŽIVANOVIĆ, S.; KOKOTOVIĆ, B.; DIMIĆ, Z.: *Compliance analysis of 5-axis vertical articulated machining robot*, 4th International Conference on Manufacturing Engineering ICMEN-Proceedings, Thessaloniki 2011, 411-422.
- [13] NOVÁK-MARCINČIN, J.; DOLIAK, M.; HLOCH, S.; ERGIĆ, T.: *Application of the virtual reality modelling language to computer aided robot control system ROANS*, Strojarstvo, 52 (2010) 2, 227-232.
- [14] MÜLLER, A.; TERZE, Z.: *Differential-geometric modelling and dynamic simulation of multibody systems*, Strojarstvo, 51 (2009) 6, 597-612.